Science of Sintering, **38** (2006) 145-153

DOI: **10.2298/SOS0602145R**

UDK 539.213:675.017.5:676.017.6

The Influence of Structural Changes on Electrical and Magnetic Characteristics of Amorphous Powder of the Ni_xMo_y Alloy

L. Ribić-Zelenović[1*)], L. Rafailović[1], M. Spasojević[1], A. Maričić[2]
[1]Faculty of Agronomy, Čačak, University of Kragujevac, Serbia
[2]Tehnical Faculty, Čačak, University of Kragujevac, Serbia

Abstract:

Nickel and molybdenum alloy powder was electrodeposited on a titanium cathode from a $NiSO_4 \cdot 7H_2O$ and $(NH_4)_6\ Mo_7O_{24} \cdot 4H_2O$ ammonium solution. The desired chemical composition, structure, size and shape of particles in the powder samples were achieved by an appropriate choice of electrolysis parameters (current density, composition and temperature of the solution, cathode material and electrolysis duration). Metal coatings form in the current density range 15 mA $cm^{-2} < j <$ 30 mA cm^{-2}. If the current density is greater than 40 mA cm^{-2} then powders form. The chemical composition of powder samples depends on the current density of electrodeposition. The molybdenum content in the powder increases with the increase of current density (in the low current density range), while in the higher current density range the molybdenum content in the alloy decreases with the increase of the current density of deposition. Smaller sized particles form at higher current density. X-ray analysis, differential scanning calorimetric and measurements of the temperature dependence of electric resistance and magnetic permeability of the powder samples were all used to establish a predominantly amorphous structure of the powder samples formed at the current density of $j \geq 70$ mA cm^{-2} . The crystalline particle content in the powder samples increases with the decrease of the current density of deposition. Powder heating causes structural changes. The process of thermal stabilization of nickel and molybdenum amorphous powders takes place in the temperature interval from 463 K to 573 K and causes a decrease in electrical resistance and increase in magnetic permeability. The crystallization temperature depends on the value of current density of powder electrodeposition. Powder formed at $j =$ 180 mA cm^{-2} begins to crystallize at 573 K, while the powder deposited at $j =$ 50 mA cm^{-2} begins to crystallize at 673 K. Crystallization of the powder causes a decrease in electric resistivity and magnetic permeability. The Curie temperature of the crystallized powders is about 10 K higher than the Curie temperature of amorphous powders.

Keywords: *Amorphous powder, Electric resistivity, Magnetic permeability.*

1. Introduction

Rapid progress in the development of new materials facilitates to a great extent development of novel technologies and modern scientific and technical progress. In recent years, a lot of new materials are obtained by sintering of powders. Metalic amorphous alloys

*)Corresponding author: lenka@tfc.kg.ac.yu

with magnetic properties are especially widely applied [1-8]. Amorphous alloys are characterized by a metastable state and when heated, the process of structural relaxation takes place in them [9-16]. The process of structural relaxation is followed by crystallization, which in turn affects mechanical, electrical, magnetic and other characteristics of these materials.

Powders of certain characteristics can be obtained by electrochemical depostion [8, 16-23]. Deposits of different chemical composition may be obtained by varying parameters like composition and temperature of the bath, cathode material and parameters of electrolysis [8, 16-23].

In this study, investigation of the influence of current density on the physical and chemical characteristics of electrochemically obtained nickel and molybdenum alloys is performed.

2. Experimental

The powder was obtained in a glass electrochemical cell with a volume of 2.0 dm^3 containing a special part with a Lugin capillary and a saturated calomel electrode. The anode used was a RuO_2/TiO_2 electrode with a 10 cm^2 surface area and the cathode was a titanium plate with a 6 cm^2 surface area and thickness of 0.2 cm. The cell was in a thermostat. The working temperature was maintained at 298 ± 1,0 K. The solution was obtained from p.a. chemicals and triple-distilled water. It contained 10.1 g dm^{-3} $NiSO_4 \cdot 7H_2O$, 1.3 g dm^{-3} $(NH_4)_6Mo_7O_{24} \cdot 4H_2O$, 0.43 g dm^{-3} NaCl, 119.6 cm^3 25% NH_4OH per dm^3. The standard electronic circuitry included a RDE 3 potentiostat Pine Instrument Co., Grove City, Pennsylvania, Hewlett Packard XY recorder and voltmetre Pro's Kit 03-9303C. The nickel and molybdenum alloy powder was deposited galvanostatically at current densities ranging from 10.0 mA cm^{-2} to 200 mA cm^{-2}. Following electrolysis, the obtained powder was washed several times with distilled water. After being washed with water, in order to prevent oxidation, the powder was washed with 0.1% benzoic acid solution and dried at 333 K. The chemical composition of the powder was determined by the atomic absorption metod. Analysis of the size and shape of powder particles was performed a by Leica Q 500MC automatic device for microstructural analysis. Investigation of electrical properties was made using samples 40x1.2x0.5mm, obtained by powder pressing under the pressure of 100 MPa. Electrical resistivity was measured by the four-point method within the temperature interval of 293 K to 973 K. The measurements were made in argon atmosphere. Differential scanning calorimetry (DSC) thermograms were obtained on a DuPontThermalAnalyser1090 at a heating rate of 20 K min^{-1} under pure argon flow. Measurements of relative magnetic permeability were performed using a modified Maxwell method, based on the action of an inhomogeneous field on the magnetic. Measurements of the magnetic force were performed with a sensitivity of 10^{-6}N. Measurements were done in argon atmosphere.

3. Results and discussion

A solution of the following composition: 101.2 g dm^{-3} $NiSO_4 \cdot 7H_2O$, 2.9 g dm^{-3} $(NH_4)_6Mo_7O_{24} \cdot 4H_2O$, 4.25 g dm^{-3} NaCl, 196,0 cm^3 25% NH_4OH per dm^3, was used to co deposit nickel and molybdenum deposits whose structure and morphology depend on the current density. If the current density is in the range 15 mA cm^{-2} < j < 30 mA cm^{-2}, the resulting deposit has a smooth compact coating of silver-white color. In the current density range from 30 mA cm^{-2} to 40 mA cm^{-2} a spongy deposit is formed. Powders are formed at a current density above 40 $mAcm^{-2}$.

The chemical composition of the powders depends on current density. Fig. 1 shows

that the Mo content increases with current density reaching its maximum at j = 70 mA cm^{-2}, but a further increase in current density decreases the Mo content in the deposits.

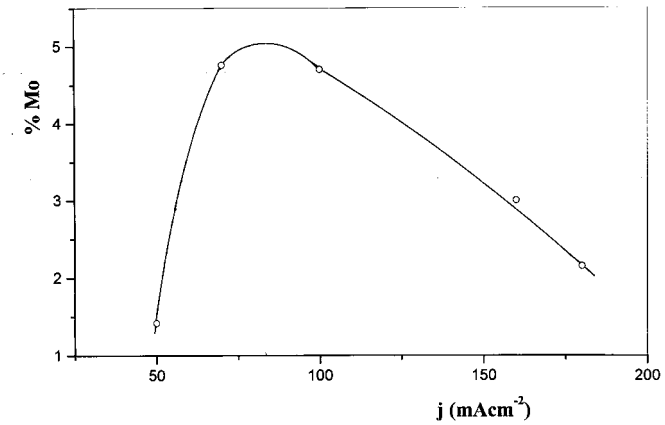

Fig. 1 Mo content (wt. %) in the alloy as a function of current density of electrodeposition

Powders formed at j < 60 mA cm^{-2} are metallic gray, while the powders obtained at j > 100 mA cm^{-2} are black.

The shape and distribution of particle sizes in the obtained powders also depend on the current density at which powders were formed. More coarse particles in the powders are formed at lower current densities (Fig. 2).

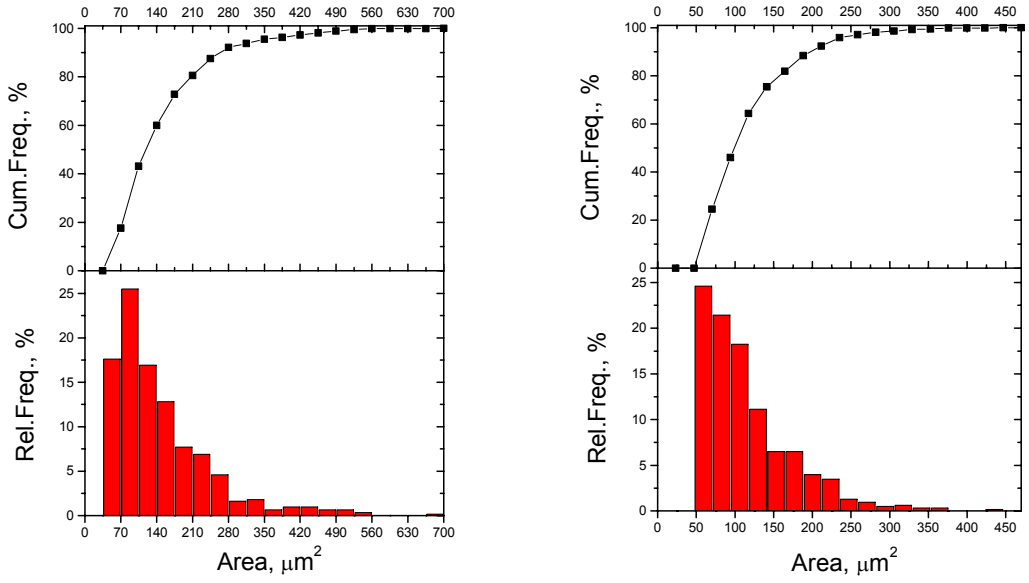

a) b)

Fig. 2 Dependence of relative and cumulative frequency of the particles' area obtained at: a) j = 70 mA cm^{-2} and b) j = 180 mA cm^{-2}

The polarization curve of the reaction of co-deposition of nickel and molybdenum indicates that in the current density range j < 7 mA cm^{-2}, the potential E is linearly dependent on the logarithm of the current density log j (dependence of Tafel) with a 60 mV slope, which in return points out that in this current density range the process is activation

controlled. Fig. 3 shows the dependence of current density of electro deposition on potential. An abrupt increase of potential with the increase in current density at current densities larger than 7 mAcm^{-2} and the existence of several shoulders along the curve, indicates a complex deposition mechanism of Ni and Mo. Nickel complexes of different compositions with ligands NH_3, OH^- and H_2O coexist in the solution. Molybdenum is present in the form of isopolimolybdats composed of different numbers of Mo_6 octaeders.

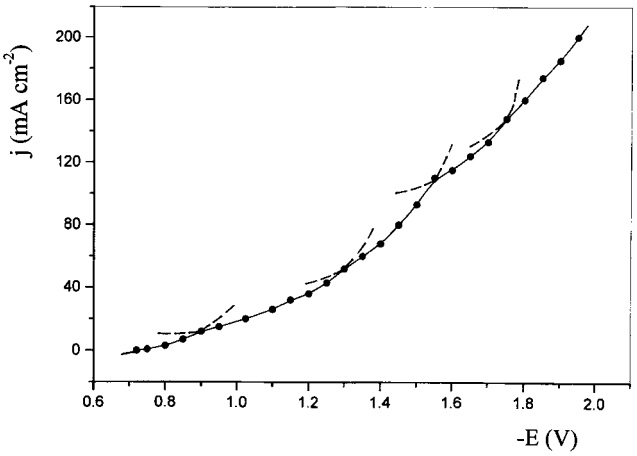

Fig. 3 Current density of electro deposition of alloys of Ni and Mo as a function of potential.

The curve shape (Fig. 3) indicates that at current densities above 10 mA cm^{-2} co deposition of Ni and Mo is a mixed controlled process. The deposition rate is determined by a chemical reaction of the electro active complex forming and diffusion of this complex towards the electrode surface. The structure of the electro active complex depends on potential. Co deposition mechanisms of Ni and Mo are different in different potential ranges, which in turn are reflected in the chemical composition, structure and morphology of the deposits.

The structure of the powders obtained at different current densities is established with X-ray analysis, differential scanning calorimetry (DSC) and measurements of magnetic permeability and electrical resistance as a function of temperature. Pronounced diffraction peaks on the X-ray diagram of the powder obtained at 50 mA cm^{-2} indicate a particle content with a crystal structure. Powders formed at higher current densities have less and less pronounced diffraction peaks with the increase in current density. The results of X-ray analysis show that powders formed at current densities $j \geq 70$ mA cm^{-2} are mostly composed of amorphous particles. The same conclusions are drawn from analysis of thermal diagrams and dependence of magnetic permeability and electrical resistance from temperature. Fig. 4 shows thermal diagrams of powders obtained at different temperatures.

Fig. 4 shows that the peak height increases with the increase in current density of powder electrodeposition. This indicates that powders obtained at higher current densities have a higher content of particles with an amorphous structure. The thermal diagrams presented show that crystallization of the powders begins at lower temperatures, if the powders were obtained at higher current densities.

Powder formed at j = 180 mA cm^{-2} begins to crystallize at 573 K, while powder obtained at j = 50 mA cm^{-2} begins to crystallize at 693 K. This indicates that powders formed at higher current densities are less stable. Crystallization of the powder causes decrease in the electrical resistance. This is illustrated by a diagram in Fig. 5. It shows that the increase in electrical resistance slows down with a temperature increase in the temperature range 693 K < T< 793 K due to partial crystallization of the powder. An abrupt decrease in the electrical resistance takes place in the temperature range 823 K < t < 973 K.

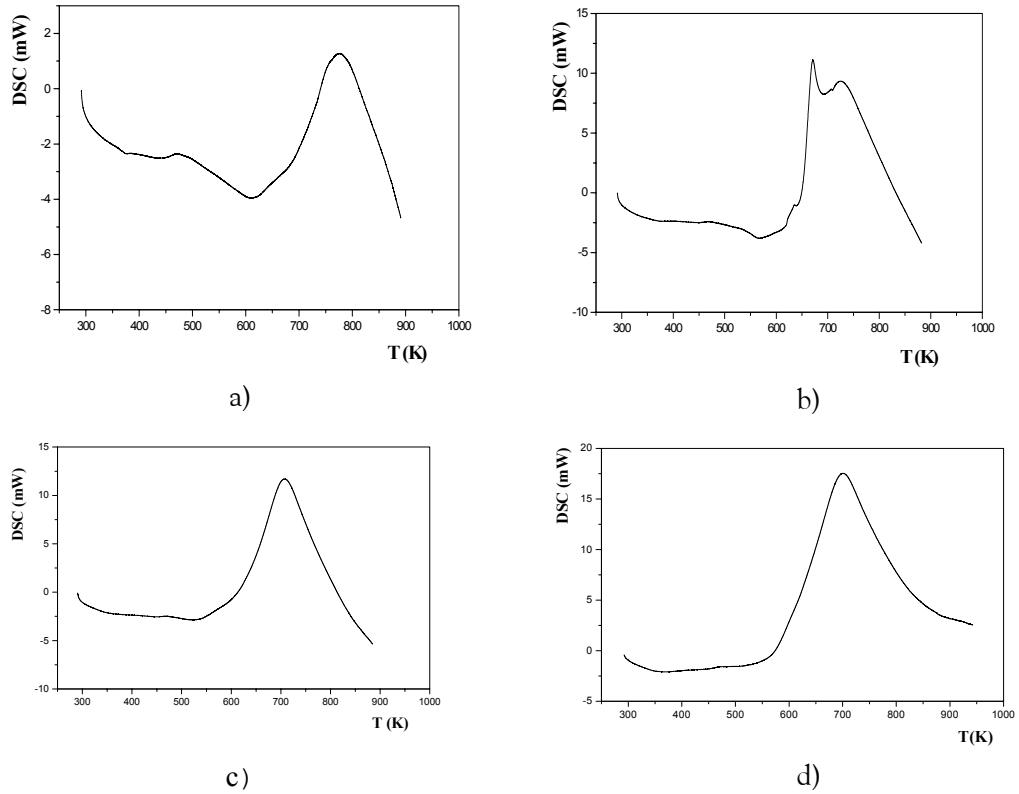

Fig. 4 DSC thermal diagrams of powders of Ni and Mo alloys obtained at different current densities: a) j = 50 mA cm^{-2} b) j = 70 mA cm^{-2} c) j = 160 mA cm^{-2} d) j = 180 mA cm^{-2}. The heating rate is 20 K min^{-1}.

In this temperature range, the powder is mostly crystallized (Fig. 4 and Fig. 5). After the powder was heated to the temperature of 953 K, it was kept at this temperature for 30 minutes in order to achieve complete crystallization of the powder. After that, the powder was cooled down and its electrical resistance was measured. The resistance decreased linearly with the decrease in temperature. Repeated heating of the powder to 953 K obtained resistance values identical to those obtained during cooling after crystallization at 953 K. This is a confirmation that the crystallization process took place in the temperature range 693 K< T< 953 K and that Ni and Mo alloy powder formed electrochemically at j =180 mA cm^{-2} has an amorphous structure. Fig. 5 shows that powder resistance increases linearly with a temperature increase in the range 293 K < T < 463 K, during initial heating of the powder. This indicates that structural changes of the powder do not take place in the same temperature range. The same conclusions are drawn from the thermal diagrams shown in Fig. 4. The resistance of the powder decreases with a temperature increase in the range 463 K < T < 573 K. In this temperature interval, a small endopeak can be noticed in the thermal diagram. This an indication that in this temperature range, crystallization does not take place, but a process of thermal stabilization of defects formed at the same time the powders were formed. In this temperature range, it is likely that a better contact among amorphous particles is achieved (which causes a decrease in electrical resistance). A linear increase in resistance in the temperature interval from 573 K to 693 K, caused by the temperature increase, indicates that in this range, significant crystallization of the amorphous powders did not take place, at a heating rate of 30 K min^{-1}. Figs. 6 and 7 show the temperature dependence of magnetic permeability of the powders formed at j = 180 mA cm^{-2} and j = 70 mA cm^{-2}. During initial heating, the relative magnetic permeability does not change significantly up to 463 K, because there are no structural changes in the powder in this temperature interval (Fig. 4 and 5). From

473 K to 573 K the relative magnetic permeability increases in the powder formed at j = 180 mA cm^{-2}, for around 25%, while the increase is about 75% for the powder formed at j = 100 mA cm^{-2}. This increase is caused by thermal stabilization.

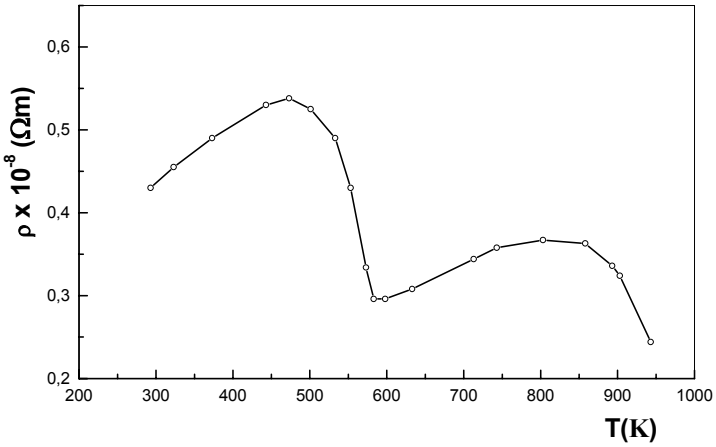

Fig. 5 Specific electrical resistance as a function temperature of the pressed powder obtained at j =180 mA cm^{-2}. The heating rate is 30 K min^{-1}.

After structural relaxation of the amorphous powders takes place at 703 K, the relative magnetic permeability of the cooled powders increased for about 25% in the former, and about 75% in the latter case. During the second heating, no significant change in the relative magnetic permeability is noticed below 613 K, since the process of thermal stabilization was completely finished during initial heating of the powders. The powders formed at lower current densities have a more pronounced endopeak (Fig. 4) and a more pronounced decrease in electrical resistance, which indicates that thermal stabilization is present more in these powders.

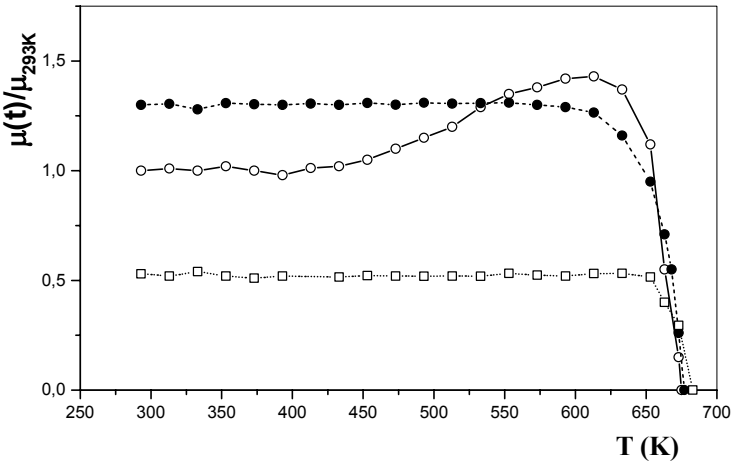

Fig. 6. Dependence of the relative magnetic permeability of the powder formed at j = 180 mA cm^{-2} from temperature: ○ – first heating, ● - second heating, □ – third heating. The heating rate is 30 K min^{-1}.

This causes that powders formed at lower current densities exhibit, after initial heating to 703 K, a larger change in relative magnetic permeability. The powders obtained at higher current densities have a larger magnetic permeability due to the larger amorphous phase content. After crystallization of the powders of nickel and molybdenum amorphous alloys at 953 K, their permeability decreases, and the obtained value does not depend on temperature in the temperature interval 293 K < T < 613 K.

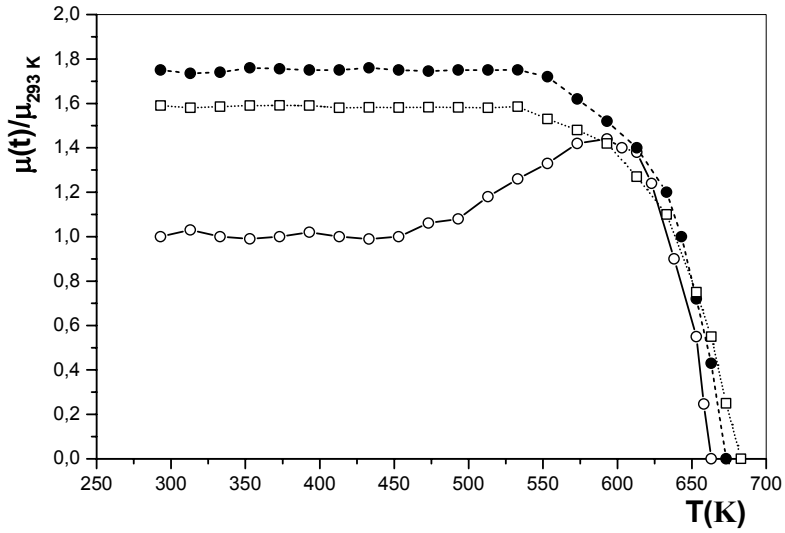

Fig. 7. Relative change in magnetic permeability of the powder formed at j = 70 mA cm^{-2} as a function of temperature: ○ – the first heating, ● - the second heating, □ – the third heating. The heating rate is 30 K min^{-1}.

Powders formed at different current densities, have approximately the same values of magnetic permeability after crystallization. The Curie temperature of the amorphous powders is about 10 K lower than the Curie temperature of crystallized powders (Figs. 6 and 7).

4. Conclusion

Nickel and molybdenum amorphous alloy powder with a well defined chemical composition, structure, size and shape of particles is obtained by an appropriate choice of electrolysis parameters, on the titanium cathode, from an $NiSO_4 \cdot 7H_2O$ and$(NH_4)_6Mo_7O_{24} \cdot 4H_2O$ ammonium solution.

Thermal stabilization of nickel and molybdenum amorphous alloy powder took place in the temperature interval from 463 K to 573 K and is followed by a decrease in electrical resistance and increase in magnetic permeability. The temperature of crystallization of nickel and molybdenum amorphous alloy powders was lower if the powder was formed at higher current density. The powder formed at j = 180 mA cm^{-2} crystallized at T >573 K, while the powder formed at j = 50 mA cm^{-2} only begins to crystallize at 673 K. Crystallization of the powder causes a decrease in its electrical resistance and magnetic permeability. The Curie temperature of crystallized powders is about 10 K higher than the Curie temperature of amorphous powders.

Acknowledgements

This work was supported by the Ministry for Science, Technology and Environmental Protection of the Republic of Serbia (Project 142011G). The authors would like to express gratitude to Academician M.M.Ristić for useful discussions.

References

1. T. R. Anantharaman, Trans. Tech., Aedermansorf, Switzerland, 1984.
2. P. Haasen and R. I. Joffe, Amorphous Metals and Semiconductors, Pergamon, London, 1986.
3. N. F. Motte and E. A. Davis, Electronic Processes in Non-Crystalline Materials, Clarendon Press, Oxford, 1979.
4. H. Steeb and H. Warlimont. Rapidly Quenched Metals, Elsevier, Amsterdam, 1985.
5. Yu. A. Kunitsky, V. I. Lisov, T. L. Tsaregradskaya, O. V. Turkov, Science of Sintering: Current problems and new trends, Beograd, 2003. p.319-328.
6. L. A. Jakobson, J. Mc. Kittrik, Rapid Solidification Processing, Elsevier, 1994.
7. M. V. Šušić, J. Mat. Sci. 22 (1987) 3011.
8. A. Maričić, M. Spasojević, L. Rafailović, V. Milovanović, L. Ribić-Zelenović, Material Science Forum, 453 (2004) 411.
9. M. V. Šušić, A. M. Maričić, Mat. Chem. And Physies, 19 (1998) 517.
10. M. V. Šušić, P. V. Budberg, S. P. Alisova, A. M. Maričić, J. Serb. Chem. Soc., 60 (1995).
11. A. M. Maričić, M. M. Ristić, Science of Sintering, 35 (2003) 31.
12. M. V. Šušić, D. Minić, A. M. Maričić, B. Jordović, Science of Sintering, 28 (1996) 105.
13. M. V. Šušić, A. M. Maričić, N. S. Mitrović, Science of Sintering, 28 (1996) 189.
14. A. M. Maričić, M. M. Ristić, Science of Sintering, 28 (1996) 182.
15. A. M. Maričić, M. V. Šušić, M. M. Ristić, J. Serb. Chem. Soc.62 (1997) 643.
16. M. Spasojević, A. Maričić, L. Rafailović, Science of Sintering, 36 (2004) 105.
17. A. R. Despić, K. I. Popov, Modern Aspects of Electrochemistry, Vol. 7. Plenum press, New York, 1972.
18. N. Ibl, Helv. Chim. Acta, 37 (1954).
19. K. I. Popov, M. G. Pavlović, Electrodeposition of Metal Powders with Controlled Particled Grains Size and Morphology in Modern Aspects of Electrochemistry, B. E. Conway, J. O'M. Bockris, R. E. White, Eds., Vol.24 Plenum, New York, 1973 pp. 299-391.
20. M. G. Pavlović, Lj. J. Pavlović, N. D. Nikolić, K. I. Popov, Materials Science Forum, 352(2000)65.
21. M. G. Pavlović, K. I. Popov, E. R. Stojiljković, Biltein of Electrochemistry, 14 (1988) 211.
22. M. G. Pavlović, Lj. J. Pavlović, E. R. Ivanović, V. Radmilović, K. I. Popov, J. Serb. Chem. Soc. 66 (2001) 923.
23. M. Spasojević, A. Maričić, L. Ribić-Zelenović, L. Rafailović, B. Jordović, J. Appl. Electrochem. in press.

Садржај: *Прах легуре никла и молибдена добијен је на титанској катоди електрохемијским таложењем из амонијачног раствора* $NiSO_4 \cdot 7H_2O$ *и* $(NH_4)_6 Mo_7O_{24} \cdot 4H_2O$*. Подесним избором параметара електролизе (густине струје, састава и температуре раствора, природе катоде и времена трајања електролизе) добијени су прахови жељеног хемијског састава, структуре, величине и облика честица. У области густина струје* $15 < j < 30$ $mAcm^{-2}$ *настају металне превлаке. Прахови настају на густинама струје већим од 40* $mAcm^{-2}$*. Хемијски састав праха зависи од густине струје таложења. Са порастом густине струје садржај молибдена у праху расте (у*

области малих густина струје), а при већим густинама струје садржај молибдена у легури опада са порастом густине струје таложења. На већим густинама струје настају ситније честице. Рендгенском анализом, диференцијалном скенирајућом калориметријом и мерењем температурне зависности електричне отпорности и магнетне пермеабилности установљено је да прахови формирани на j ≥70 mAcm^{-2} имају претежно аморфну структуру. Садржај кристалних честица у праховима расте са смањењем густине струје таложења. Загревањем прахова долази до структурних промена. Процес термичке стабилизације аморфних прахова никла и молибдена одвија се у температурном интервалу од 463 до 573 K и условљава пад електричне отпорности и пораст магнетне пермеабилности. Температура кристализације зависи од густине струје формирања прахова. Прах формиран на j = 180 mAcm^{-2} почиње да кристализује на 573 K, док прах депонован на j = 50 mAcm^{-2} почиње да кристализује тек на 673 K. Кристализација праха условљава смањење електричне отпорности и магнетне пермеабилности, Киријева температура искристалисаних прахова је за око 10K виша од Киријеве температуре аморфних прахова.

Кључне речи: *Аморфни прах, електрична отпорност, магнетна пермеабилност.*